

# Identification of ML204, a Novel Potent Antagonist That Selectively Modulates Native TRPC4/C5 Ion Channels\*<sup>[5]</sup>

Received for publication, June 22, 2011, and in revised form, July 21, 2011. Published, JBC Papers in Press, July 27, 2011, DOI 10.1074/jbc.M111.274167

Melissa Miller<sup>†1</sup>, Jie Shi<sup>†1</sup>, Yingmin Zhu<sup>§</sup>, Maksym Kustov<sup>¶</sup>, Jin-bin Tian<sup>§</sup>, Amy Stevens<sup>‡</sup>, Meng Wu<sup>‡</sup>, Jia Xu<sup>‡</sup>, Shunyou Long<sup>‡</sup>, Pu Yang<sup>§</sup>, Alexander V. Zholos<sup>¶</sup>, James M. Salovich<sup>||\*\*††</sup>, C. David Weaver<sup>||</sup>, Corey R. Hopkins<sup>||\*\*††2</sup>, Craig W. Lindsley<sup>||\*\*††</sup>, Owen McManus<sup>‡</sup>, Min Li<sup>‡2</sup>, and Michael X. Zhu<sup>§</sup>

From the <sup>†</sup>Department of Neuroscience, High Throughput Biology Center, and Johns Hopkins Ion Channel Center, Johns Hopkins University School of Medicine, Baltimore, Maryland 21205, the <sup>§</sup>Department of Integrative Biology and Pharmacology, Medical School, University of Texas Health Science Center at Houston, Houston, Texas 77030, the <sup>¶</sup>Centre for Vision and Vascular Science, School of Medicine, Dentistry, and Biomedical Sciences, Queen's University Belfast, Belfast BT12 6BA, Northern Ireland, United Kingdom, the <sup>||</sup>Department of Pharmacology and <sup>\*\*</sup>Vanderbilt Center for Neuroscience Drug Discovery, Vanderbilt University Medical Center, Nashville, Tennessee 37232, and the <sup>††</sup>Department of Chemistry, Vanderbilt Specialized Chemistry Center for Accelerated Probe Development (Molecular Libraries Probe Production Centers Network), Nashville, Tennessee 37232

Transient receptor potential canonical (TRPC) channels are Ca<sup>2+</sup>-permeable nonselective cation channels implicated in diverse physiological functions, including smooth muscle contractility and synaptic transmission. However, lack of potent selective pharmacological inhibitors for TRPC channels has limited delineation of the roles of these channels in physiological systems. Here we report the identification and characterization of ML204 as a novel, potent, and selective TRPC4 channel inhibitor. A high throughput fluorescent screen of 305,000 compounds of the Molecular Libraries Small Molecule Repository was performed for inhibitors that blocked intracellular Ca<sup>2+</sup> rise in response to stimulation of mouse TRPC4 $\beta$  by  $\mu$ -opioid receptors. ML204 inhibited TRPC4 $\beta$ -mediated intracellular Ca<sup>2+</sup> rise with an IC<sub>50</sub> value of 0.96  $\mu$ M and exhibited 19-fold selectivity against muscarinic receptor-coupled TRPC6 channel activation. In whole-cell patch clamp recordings, ML204 blocked TRPC4 $\beta$  currents activated through either  $\mu$ -opioid receptor stimulation or intracellular dialysis of guanosine 5'-3-O-(thio)triphosphate (GTP $\gamma$ S), suggesting a direct interaction of ML204 with TRPC4 channels rather than any interference with the signal transduction pathways. Selectivity studies showed no appreciable block by 10–20  $\mu$ M ML204 of TRPV1, TRPV3, TRPA1, and TRPM8, as well as KCNQ2 and native voltage-gated sodium, potassium, and calcium channels in mouse dorsal root ganglion neurons. In isolated guinea pig ileal myocytes, ML204 blocked muscarinic cation currents activated by bath application of carbachol or intracellular infusion of GTP $\gamma$ S, demonstrating its effectiveness on native TRPC4 currents. Therefore, ML204 represents an excellent novel tool for

investigation of TRPC4 channel function and may facilitate the development of therapeutics targeted to TRPC4.

Transient receptor potential (TRP)<sup>3</sup> channels have emerged as molecular sensors of extracellular and intracellular environmental changes (1). These channels are widely present in all species across the animal kingdom, and they serve diverse functional roles in different tissue/cell types. Mammalian TRP channels are categorized into six subfamilies, TRPC (canonical), TRPV (vanilloid), TRPM (melastatin), TRPA (ankyrin), TRPP (polycystin), and TRPML (mucolipin), based on sequence similarities (2). Among these subfamilies, TRPC channels share closest similarity with the archetypical TRP channel originally identified as responsible for the *trp* phenotype of *Drosophila* phototransduction. Like the *Drosophila* TRP and TRP-like channels, mammalian TRPC channels are Ca<sup>2+</sup>-permeable nonselective cation channels activated downstream from the stimulation of phospholipase C pathways via, typically, G protein-coupled receptors (GPCRs) and/or receptor tyrosine kinases (3). However, the precise step or component of the phospholipase C pathway that serves as the ultimate trigger of TRPC channel activation remains a matter of debate. Recently, coincident phosphoinositide hydrolysis and local acidification by the action of phospholipase C have been suggested to underlie activation of *Drosophila* TRP and TRP-like channels (4). The generality of this mechanism for mammalian TRPC channels remains to be demonstrated.

The seven mammalian TRPC proteins are further divided into four subgroups, TRPC1, TRPC2, TRPC3/C6/C7, and TRPC4/C5, based on sequence similarities. TRPC2, C3, C6, and C7 can be directly activated by diacylglycerols, including a synthetic analog, 1-oleoyl-2-acetyl-*sn*-glycerol (OAG) (5), but this

\* This work was supported, in whole or in part, by National Institutes of Health, MLPCN, Grants U54MH084691 (to M. L.), U54MH084659 (C. W. L.), and R21NS056942 (to M. X. Z.). Vanderbilt is a member of the MLPCN and houses the Vanderbilt Specialized Chemistry Center for Accelerated Probe Development. Johns Hopkins is a member of the MLPCN and houses the Johns Hopkins Ion Channel Center.

<sup>[5]</sup> The on-line version of this article (available at <http://www.jbc.org>) contains supplemental Figs. S1 and S2 and Tables S1 and S2.

<sup>1</sup> Both authors contributed equally to this work.

<sup>2</sup> To whom correspondence may be addressed. E-mail: minli@jhmi.edu and corey.r.hopkins@vanderbilt.edu.

<sup>3</sup> The abbreviations used are: TRP, transient receptor potential; GTP $\gamma$ S, guanosine 5'-3-O-(thio)triphosphate; MLPCN, Molecular Libraries Probe Production Centers Network; MLSMR, Molecular Libraries Small Molecule Repository; GPCR, G protein-coupled receptor; OAG, 1-oleoyl-2-acetyl-*sn*-glycerol; m<sub>1</sub>CAT, muscarinic receptor-activated cation currents; ACh, acetylcholine; SAR, structure-activity relationship; pF, picofarad;  $\mu$ -OR,  $\mu$ -opioid receptor(s); DAMGO, [D-Ala<sup>2</sup>, N-MePhe<sup>4</sup>, Gly-ol]-enkephalin.

stimulation may be partial because more elevated channel activation is achieved with receptor stimulation and/or combined stimulation by diacylglycerol and inositol 1,4,5-trisphosphate receptors (6). TRPC4/C5 channels are not activated by diacylglycerol but are facilitated by internal and external  $\text{Ca}^{2+}$  (7). Activation by the  $\text{G}\alpha_i$  pathway has also been proposed as a mechanism specific for TRPC4 because other tested TRPC channels seem to be unaffected when constitutively active  $\text{G}\alpha_{i2}$  is expressed (8). Other proposed activation mechanisms include internal  $\text{Ca}^{2+}$  store depletion (9, 10) and extracellular application of 10–100  $\mu\text{M}$  lanthanides (11, 12). However, these responses are conditional, depending upon variables that have not been clearly defined.

A number of physiological functions have been assigned to TRPC4 channels based on the studies of TRPC4 knock-out mice, including regulation of agonist-dependent vasorelaxation in aortic endothelial cells (9), actin-stress fiber formation and microvascular permeability in lung vascular endothelial cells (13), serotonin-induced dendritic release of  $\gamma$ -aminobutyric acid in thalamic interneurons (14), and muscarinic receptor-activated cation currents ( $\text{mI}_{\text{CAT}}$ ) in visceral smooth muscles, which modulate intestinal contraction and motility (15–17). However, functional characterization of these channels in native tissues has been hampered by a lack of specific pharmacological tools. SKF96365 and 2-aminoethoxydiphenyl borate (2-APB), as well as lanthanum and gadolinium, can modulate TRPC4/C5 functions, but they act on a number of other channels with comparable potency. In fact, no specific small molecule inhibitors for TRPC4 or TRPC5 have been reported to date.

Using a cell-based high throughput fluorescence assay, we have screened 305,000 compounds of the Molecular Libraries Small Molecule Repository (MLSMR) available to the Molecular Libraries Probe Production Centers Network (MLPCN). After characterization and optimization studies, here we report a novel, potent, and relatively selective antagonist of TRPC4 and TRPC5 channels.

## EXPERIMENTAL PROCEDURES

**Cell Lines and Cell Culture**—HEK293 cells were grown in DMEM (high glucose) supplemented with 10% heat-inactivated fetal bovine serum (FBS), 100 units/ml penicillin, and 100  $\mu\text{g}/\text{ml}$  streptomycin at 37 °C, 5%  $\text{CO}_2$ . Stable cell lines that express hemagglutinin (HA)-tagged mouse TRPC6 have been described (18). The stable cell line that expresses human TRPA1 in an inducible manner and the conditions for induction have been described (19). Stable cell lines that express mouse TRPC4 $\beta$ , TRPC5, TRPV3, or TRPM8 were established after transfection using Lipofectamine 2000 and selection in the medium supplemented with G418 (400  $\mu\text{g}/\text{ml}$ ; Invitrogen). Detailed procedures for transfection, selection, limiting dilution, and functional analysis of stable cell lines have been described previously (20). For stable cell lines co-expressing TRPC4 or TRPC5 and G protein-coupled receptors,  $\mu$ -opioid receptors ( $\mu$ -OR),  $\text{M}_2$  muscarinic receptors, or 5HT $_{1A}$  serotonin receptors, the receptor cDNA was placed in the pIREShygro2 vector (Clontech), and cell lines were selected in the medium containing 400  $\mu\text{g}/\text{ml}$  G418 and 100  $\mu\text{g}/\text{ml}$  hygromycin B (Calbiochem).

**Isolation and Culture of Dorsal Root Ganglion Neurons and Ileal Smooth Muscle Cells**—Dorsal root ganglion neurons were isolated from C57BL/6 mice (male and female, 6–20 weeks) and cultured for 1–2 days in DMEM (high glucose) medium following the protocol as described (21). Single smooth muscle myocytes were enzymatically isolated from the longitudinal muscle layer of the guinea pig ileum as described previously and used on the same day (22).

**Fluorescence  $\text{Ca}^{2+}$  and Membrane Potential Assays**—For primary screens, a stable HEK293 cell line co-expressing mouse TRPC4 $\beta$  and  $\mu$ -OR was grown into large batches, and frozen stocks were made so that all cells used for screening had undergone identical cell culture manipulations. For the screening assay, cells were thawed, and an equal number of cells (15,000 cells/50  $\mu\text{l}$ ) were added to each well of the 384-well assay plates (BD polylysine-precoated). Cells were maintained in culture medium without antibiotics at 37 °C, 5%  $\text{CO}_2$  for 16–18 h. For assay, cells were loaded with Fluo4-AM (2  $\mu\text{M}$ ) for 45 min at room temperature and washed once in an assay buffer composed of 1 $\times$  Hanks' balanced salt solution (containing  $\text{Ca}^{2+}$  and  $\text{Mg}^{2+}$ ) with 20 mM HEPES at pH 7.4. The primary screen assays were run using a Hamamatsu FDSS6000 kinetic imaging plate reader with excitation and emission wavelengths set to 480 and 540 nm, respectively. Test compounds were added at 5 s at 75  $\mu\text{M}$  for a final concentration of 10  $\mu\text{M}$ . At 110 s, an  $\text{EC}_{20}$  concentration of [D-Ala $^2$ , N-MePhe $^4$ , Gly-ol]-enkephalin (DAMGO) (final concentration of 1.8 nM) was added, followed by the addition of DAMGO ( $\text{EC}_{\text{max}}$ ) to a final concentration of 1.8  $\mu\text{M}$  at 215 s. Secondary and counter screening utilized the same assay technique with TRPC4 $\beta$ - and  $\mu$ -OR-expressing HEK293 cells along with parental HEK293 cells except that after wash, cells were allowed to incubate with test compounds for 20 min prior to application of  $\text{EC}_{\text{max}}$  of DAMGO.

Assessment of specificity against TRPC6 was determined using a TRPC6-expressing HEK293 cell line. The FLIPR Membrane Potential dye (Molecular Devices) was used to monitor membrane potential changes upon stimulation by acetylcholine (ACh). Similarly as for TRPC4, TRPC6-expressing cells were thawed 16–18 h prior to assay. An equal number of cells (15,000 cells/50  $\mu\text{l}$ ) were added to each well of a 384-well assay plate (BD polylysine-precoated) and grown in culture medium without antibiotics at 37 °C, 5%  $\text{CO}_2$ . Cells were then incubated with FLIPR Membrane Potential dye (prepared per the manufacturer's recommendations) for 45 min at room temperature. Plates were run using a Hamamatsu FDSS6000 kinetic imaging plate reader where test compounds were added after 5 s at 75  $\mu\text{M}$  for a final concentration within the well of 10  $\mu\text{M}$ . At 110 s, an  $\text{EC}_{\text{max}}$  concentration of ACh (60  $\mu\text{M}$ ) was added.

For tertiary assays and selectivity tests on other TRP channels, HEK293 cells stably expressing each channel type were seeded in 96-well plates precoated with polyornithine at 100,000 cells/well. Cells were loaded with Fluo4-AM to monitor intracellular  $\text{Ca}^{2+}$  changes with the use of a FlexStation microplate reader (Molecular Devices) following previously described protocols (23, 24). Rat TRPV1 was transiently transfected into HEK293 cells in the 96-well plate and used for  $\text{Ca}^{2+}$  assay 20 h post-transfection as described (23). Extracellular solution for all FlexStation assays contained 140 mM NaCl, 5.4

## ML204 Selectively Modulates Native TRPC4/C5 Channels

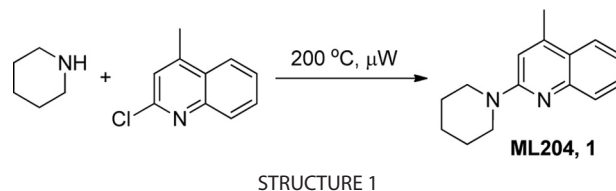
mM KCl, 1.8 mM CaCl<sub>2</sub>, 1 mM MgCl<sub>2</sub>, 10 mM glucose, and 15 mM HEPES, pH 7.4 adjusted with NaOH. Probenecid (2 mM) was included in all Ca<sup>2+</sup> assays except for TRPV1. Assays were run at room temperature (~22 °C).

**Automated Electrophysiological Recording**—HEK293 cells stably expressing TRPC4β and μ-OR were seeded in T75 flasks 2 days before testing on a QPatch16 automated patch clamp system (Sophion Biosciences). The Cs-Asp internal solution contained 150 mM cesium aspartate, 2 mM MgCl<sub>2</sub>, 0.36 mM CaCl<sub>2</sub>, 1 mM EGTA, 4 mM MgATP, 0.3 mM NaGTP, and 10 mM HEPES, pH 7.2, with CsOH (with an estimated free [Ca<sup>2+</sup>]<sub>i</sub> = 100 nM); the external solution contained 150 mM NaCl, 4 mM KCl, 2 mM CaCl<sub>2</sub>, 1 mM MgCl<sub>2</sub>, 10 mM HEPES, and 10 mM D-glucose, pH 7.4, with NaOH (25). Cells were detached into single cell suspension and allowed to recover for at least 1 h before running in single-hole mode on QPatch. Whole cell currents were filtered at 1 kHz (4-pole Bessel filter) and sampled at 5 kHz. The series resistance was compensated by 80% with a cut-off frequency of 0.8 kHz.

TRPC4 currents were elicited by a voltage protocol consisting of a 50-ms voltage step from the 0 mV holding potential to -100 mV, followed by a 110-ms voltage ramp to +120 mV, 8 ms at +120 mV, and then a step back to 0 mV for 180 ms. The voltage protocol was applied every 5 s.

**Manual Electrophysiological Studies**—HEK293 cells heterologously expressing TRPC channels were seeded in 35-mm dishes 1 day before whole-cell recordings were performed. Recording pipettes were pulled from micropipette glass (World Precision Instruments Inc., Sarasota, FL) to 2–4 megaohms when filled with a pipette solution containing 140 mM CsCl, 0.6 mM MgCl<sub>2</sub>, 1 mM EGTA, and 10 mM HEPES, pH 7.2, and placed in the bath solution, containing 140 mM NaCl, 5 mM KCl, 2 mM CaCl<sub>2</sub>, 1 mM MgCl<sub>2</sub>, 10 mM glucose, and 10 mM HEPES, pH 7.4. Isolated cells were voltage-clamped in the whole-cell mode using an EPC9 (HEKA Instruments Inc., Bellmore, NY) amplifier. Voltage commands were made from the Pulse+Pulse Fit program (version 8.53; HEKA), and currents were recorded at 5 kHz. Voltage ramps of 100 ms to -100 mV after a brief (20-ms) step to +100 mV from holding potential of 0 mV were applied every 0.5 s. Cells were continuously perfused with the bath solution through a gravity-driven multioutlet device with the desired outlet placed about 50 μm away from the cell being recorded. Drugs were diluted in the external solutions to the desired final concentrations and applied to the cell through perfusion.

Dorsal root ganglion neurons were seeded on polyornithine-coated glass coverslips and cultured. To record voltage-gated Na<sup>+</sup> and Ca<sup>2+</sup> channel currents, the pipette solution contained 117 mM CsCl, 1.8 mM MgCl<sub>2</sub>, 9 mM HEPES, 9 mM EGTA, 14 mM Tris-creatine PO<sub>4</sub>, 4 mM MgATP, and 0.3 mM TrisGTP, pH 7.4 (with CsOH). The bath solution for recording Na<sup>+</sup> channels contained 30 mM NaCl, 30 mM triethanolamine chloride, 65 mM choline chloride, 2 mM CoCl<sub>2</sub>, 5 mM MgCl<sub>2</sub>, 10 mM HEPES, and 10 mM glucose, pH 7.4 (with NaOH). The bath solution for recording Ca<sup>2+</sup> channels contained 140 mM choline chloride, 5 mM KCl, 2 mM CaCl<sub>2</sub>, 1 mM MgCl<sub>2</sub>, 10 mM HEPES, and 10 mM glucose, pH 7.4 (with KOH). To record voltage-gated K<sup>+</sup> channels, the pipette solution contained 130 mM potassium meth-



anesulfonate, 7 mM KCl, 10 mM HEPES, 0.05 mM EGTA, 1 mM Na<sub>2</sub>ATP, 3 mM MgATP, and 0.5 mM Na<sub>2</sub>GTP, pH 7.4 (with KOH). The bath solution was the same as that for Ca<sup>2+</sup> channels except that 2 mM CaCl<sub>2</sub> was replaced by 2 mM CoCl<sub>2</sub>. Isolated cells were voltage-clamped in the whole-cell mode using EPC9 and Pulse+Pulse Fit, and currents were recorded at 10 kHz. After establishing the whole-cell configuration, the cell was held at -70 mV. Voltage steps of 50 ms from -70 mV to +40 mV with a 10-mV increment were applied to elicit voltage-gated Na<sup>+</sup> and Ca<sup>2+</sup> currents. Voltage steps of 300 ms from -70 to +40 mV with a 10-mV increment following a prepulse from -70 to -110 mV for 50 ms were applied to elicit voltage-gated K<sup>+</sup> currents.

For whole-cell recording of ileal smooth muscle myocytes, the external solution contained 120 mM CsCl, 12 mM glucose, and 10 mM HEPES, pH 7.4 adjusted with CsOH. The pipette solution contained 80 mM CsCl, 1 mM MgATP, 5 mM creatine, 0.2 mM GTPγS, 5 mM D-glucose, 10 mM HEPES, 10 mM BAPTA, and 4.6 mM CaCl<sub>2</sub> ([Ca<sup>2+</sup>]<sub>i</sub> = 100 nM), pH 7.4 adjusted with CsOH. Carbachol-induced currents were recorded with 1 mM GTP instead of GTPγS in order to minimize current desensitization (22). Currents were recorded using borosilicate patch pipettes (2–3 megaohms) and an Axopatch 200B amplifier (Molecular Devices, Union City, CA) interfaced to Digidata 1322A with the pClamp 9 support. Holding potential was -40 mV. Parallel continuous data acquisition was performed using MiniDigi 1A (Molecular Devices) and AxoScope 9 software. *mI*<sub>CAT</sub> were induced either by external application of carbachol (100 μM, which is EC<sub>max</sub>) or by infusing 200 μM GTPγS via the patch pipette. Data were analyzed and plotted using Clampfit 9 (Molecular Devices) and Origin 8.0 (Microcal, Northampton, MA). The steady-state current-voltage (*I*-*V*) relationships were measured by slow (6-s) voltage ramps from -80 to +120 mV. All whole-cell experiments were performed at room temperature (~22 °C).

**Probe Preparation (Structure 1)**—The chloroquinoline (100 mg, 0.56 mmol) and piperidine (0.22 ml, 2.25 mmol) were stirred in a microwave reaction vial. The vial was sealed and then irradiated under microwave at 200 °C with stirring for 15 min. LC/MS indicated reaction completion. The reaction mixture was diluted with MeOH and then concentrated under vacuum. The residue was dissolved in 3% aqueous HCl (10 ml) and washed with dichloromethane (2 × 5 ml). The aqueous layer was treated with 2 N NaOH until the pH was 8, resulting in a white slurry. The slurry was extracted with dichloromethane (3 × 20 ml). The combined organic layers were dried over Na<sub>2</sub>SO<sub>4</sub> and concentrated to give 70 mg (55%) of the product as a white solid. <sup>1</sup>H NMR (400 MHz, DMSO-*d*<sub>6</sub>): δ 7.75 (d, *J* = 8.1 Hz, 1H), 7.52–7.45 (m, 2H), 7.21–7.17 (m, 1H), 7.10 (s, 1H), 3.67 (bs, 4H), 2.54 (s, 3H), 1.62–1.55 (m, 6H). LC/MS: R<sub>T</sub> = 0.65 min, *m/z* = 227.2 [M + H]<sup>+</sup>.

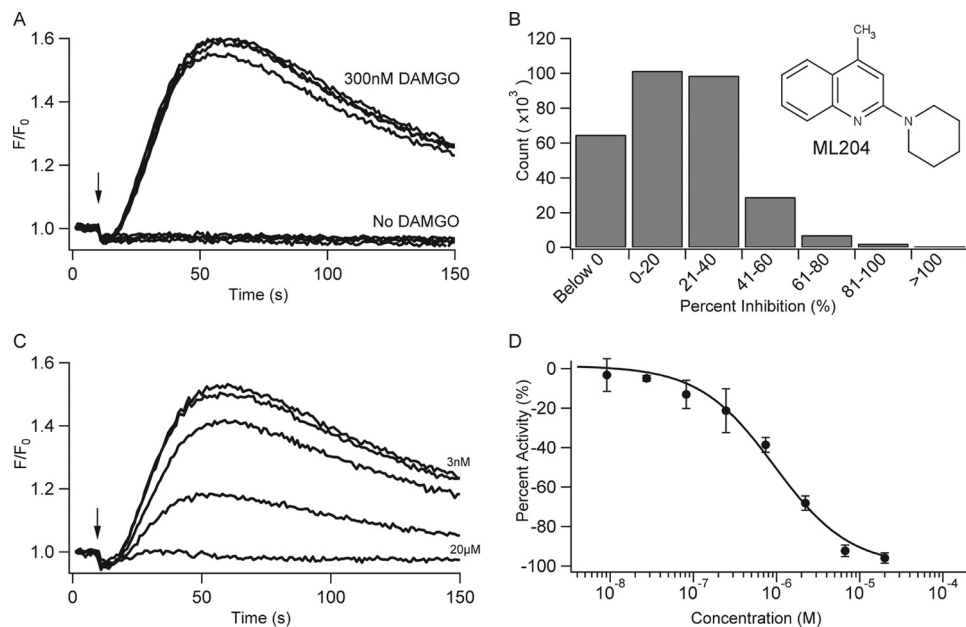


**FIGURE 1. Fluorescent assay for TRPC4 $\beta$  channels used to identify and characterize ML204.** *A*, calcium mobilization signals in a HEK293 cell line co-expressing recombinant mouse TRPC4 $\beta$  channel and the  $\mu$ -opioid receptor with (upper traces) or without (lower traces) stimulation by DAMGO (300 nM). The vertical arrow indicates the time of solution addition. *B*, chemical structure of ML204. *C*, multiple-well overlay of representative traces for the inhibition of DAMGO-induced calcium mobilization in the presence of ML204 (3 nM, 27 nM, 247 nM, 2.22  $\mu$ M, and 20  $\mu$ M). *D*, concentration-dependent inhibition of calcium flux by ML204; each point was run in quadruplicate, and the averages  $\pm$  S.D. (error bars) are plotted.  $IC_{50}$  for individual experiment shown equals 0.99  $\mu$ M.

## RESULTS

The Johns Hopkins Ion Channel Center and the Vanderbilt Specialized Chemistry Center are members of the MLPCN, which is a consortium that provides high throughput small molecule screening and medicinal chemistry support for identification of chemical probes for use as tools to explore biological targets and pathways for which available small molecule tools are inadequate. Within this network and in collaboration with external investigators, a fluorescent assay was used to screen the 305,000 compounds of the MLSMR to identify inhibitors of TRPC4 channels. The primary screening assay utilized an approach in which TRPC4 $\beta$  channels were activated by application of a  $\mu$ -opioid receptor agonist, DAMGO, as described below. The results of the primary screen were released in PubChem (AID2247 and AID2256), where the criteria for selecting active compounds were detailed. The active compounds were ordered and retested for activity in the primary screens. Based on activity, chemical scaffold, and counter screens, SID 24829278 (CID 230710) was identified in the primary screen, resynthesized (SID 97362164, VU0024172-3) and confirmed as a TRPC4 $\beta$  inhibitor. Structure-activity relationship (SAR) studies coupled with biological characterization led to nomination of CID 24829278 as a Molecular Libraries Probe compound, ML204. This compound is available to the public from Evotec OAI.

**High Throughput Screen Using Fluorescence-based Detection of TRPC4 $\beta$  Activity**—A fluorescence-based assay to monitor changes in intracellular calcium concentrations ( $[Ca^{2+}]_i$ ) was developed to follow the TRPC4 $\beta$  activity. DAMGO was applied to cells co-expressing recombinant TRPC4 $\beta$  channels and the  $\mu$ -OR. Changes in  $[Ca^{2+}]_i$  were monitored through use of a  $Ca^{2+}$  sensitive dye (Fluo-4AM) and recorded on a Hamamatsu FDSS6000 plate reader. Application of 300 nM DAMGO was

used to activate the  $\mu$ -OR and trigger TRPC4 $\beta$  opening via the  $G_{i/o}$ -coupled pathway (20). Representative traces of different wells corresponding to application of 300 nM DAMGO or buffer alone are shown in Fig. 1A, indicating a large and consistent signal window. In this format, the assay afforded a  $Z'$  factor of  $0.64 \pm 0.15$  ( $n = 961$ ), indicating a robust assay format. DAMGO did not trigger a change in  $[Ca^{2+}]_i$  in cells expressing  $\mu$ -OR but lacking TRPC4 $\beta$  channels, as similarly described (20). This assay was utilized to screen the MLSMR collection of 305,000 compounds at a 10  $\mu$ M concentration for inhibitors of  $[Ca^{2+}]_i$  rise, and summary results are shown in Fig. 1B. From the initial screen, 856 compounds were selected for further confirmation based on the structure and potency. Confirmed active compounds were further evaluated for inhibition of TRPC4 $\beta$  activated via 5HT $_{1A}$  receptors to exclude compounds that acted at the  $\mu$ -OR (data not shown). From this set, ML204 was selected for in depth investigation based on preliminary selectivity and potency assessment.

Fig. 1C shows representative kinetic traces of DAMGO-evoked  $[Ca^{2+}]_i$  changes in cells co-expressing TRPC4 $\beta$  and  $\mu$ -OR in the presence of increasing concentrations of ML204 (from 3 nM to 20  $\mu$ M; see figure legends). Complete inhibition of TRPC4 $\beta$ -mediated  $[Ca^{2+}]_i$  rise was achieved at 20  $\mu$ M ML204. The concentration for 50% inhibition ( $IC_{50}$ ) was  $0.96 \pm 0.26$   $\mu$ M in replicate experiments ( $n = 5$ ).

**ML204 Blocks TRPC4 Currents Activated by Agonist Stimulation of  $\mu$ -OR in Electrophysiological Experiments**—To evaluate the inhibitory effects of ML204 on TRPC4 $\beta$  channels, an electrophysiological assay was established on the QPatch16 automated electrophysiology instrument. Whole-cell voltage clamp recordings were made from the TRPC4 $\beta$ - and  $\mu$ -OR-co-expressing HEK293 cells that were used in the primary, confirmatory, and SAR assays. In the presence of  $\mu$ -OR agonist,

## ML204 Selectively Modulates Native TRPC4/C5 Channels

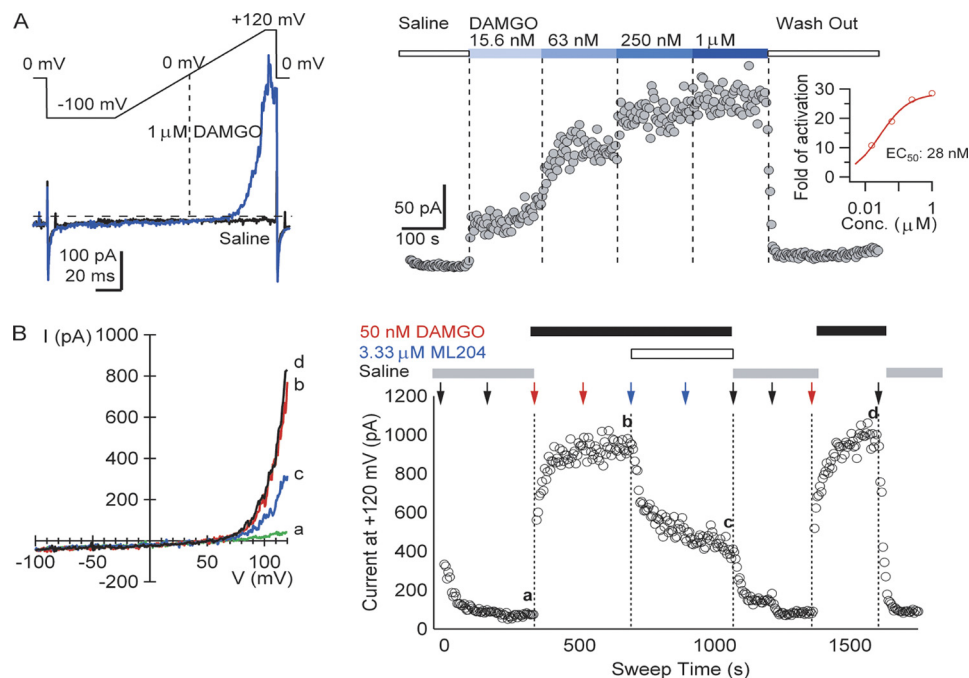


**FIGURE 2. Activation of heterologously expressed TRPC4 channels and its inhibition by ML204.** *A*, TRPC4 currents evoked by stimulation of  $\mu$ -OR with 1  $\mu$ M DAMGO were elicited by 110-ms voltage ramps from  $-100$  to  $+120$  mV, applied every 5 s from a holding potential of 0 mV. *Left*, ramp currents recorded before (*black*) and after the addition of 1  $\mu$ M DAMGO (*blue*). The horizontal dashed line indicates zero current level. *Right*, DAMGO caused dose-dependent increases in TRPC4 $\beta$  currents. After ramping up to  $+120$  mV, the cells were held at  $+120$  mV for 8 ms, and the average current amplitude at  $+120$  mV was plotted versus time. The inset displays a Hill plot with the slope fixed to one of the normalized increases of TRPC4 $\beta$  currents versus DAMGO concentration. *B*, inhibition of DAMGO-induced TRPC4 $\beta$  currents by ML204. The same voltage protocol as in *A* was used. *Left*, currents before (*a*) and after 50 nM DAMGO addition (*b*), with 3.33  $\mu$ M ML204 and 50 nM DAMGO (*c*), and after washout (*d*). *Right*, time course of TRPC4 $\beta$  current block by 3.33  $\mu$ M ML204 after activation by 50 nM DAMGO. Solutions were added twice for each condition, as indicated by vertical arrows.

DAMGO, TRPC4 currents were recorded using voltage ramps with an internal solution containing cesium aspartate to minimize background potassium and chloride currents (Fig. 2*A*). The outwardly rectifying currents (*blue trace* in Fig. 2*A*, *left*) observed in response to DAMGO are characteristic of TRPC4 $\beta$  channels when they are weakly activated (7). The inward currents at negative membrane potentials were very small, and channel activation was more readily observed at depolarized voltages ( $>50$  mV) and was dependent on the doses of DAMGO applied (Fig. 2*A*, *right*). Complete recovery of TRPC4 $\beta$  currents to base-line levels after high doses ( $>1$   $\mu$ M) of DAMGO was not always achieved, and, as a result, application of high doses of DAMGO to achieve clear saturation of maximal effects was not routinely carried out in titration experiments. Given this limitation, the estimated EC<sub>50</sub> for DAMGO activation of TRPC4 $\beta$  currents in the described assay was  $22.0 \pm 13.4$  nM ( $n = 10$ ). Thus, 50 nM DAMGO was used as the stimulus in the following automated electrophysiological assays. The currents activated by 50 nM DAMGO remained stable for 20 min (data not shown), affording a sufficient time window to test the effects of ML204 on TRPC4 $\beta$  currents.

Inhibition of TRPC4 $\beta$  currents by 3.33  $\mu$ M ML204 is shown in Fig. 2*B*. After the formation of whole-cell configuration, cells were stabilized in saline for 5 min before the addition of 50 nM DAMGO. The response at negative potentials was small (Fig. 2*B*, *a*); the current amplitude at  $+120$  mV after 50 nM DAMGO addition reached a plateau value of  $\sim 900$  pA in 3 min (Fig. 2*B*, *left*). This is consistent with TRPC4 activation by membrane depolarization, in addition to GPCR- and Ca<sup>2+</sup>-dependent pro-

cesses. A second application of 50 nM DAMGO did not further enhance the current amplitude, indicating adequate solution exchange. Two additions of 3.33  $\mu$ M ML204 reduced the current amplitude by more than 50%. The remaining currents were completely washed out by two applications of saline. Reapplication of 50 nM DAMGO produced currents of the same amplitudes as before ML204 inhibition. Multiple concentrations of ML204 were tested using this single-dose titration scheme in separate experiments, yielding an IC<sub>50</sub> of 2.9  $\mu$ M ( $n = 7$ ). A revised compound addition protocol using the same voltage protocol, which allows higher throughput compound testing, was examined. After activation of TRPC4 currents with 50 nM DAMGO, three ascending concentrations of ML204 were sequentially applied to the same cell in the presence of 50 nM DAMGO. Dose-dependent inhibition of the TRPC4 $\beta$  currents was observed (data not shown) with an IC<sub>50</sub> of  $3.55 \pm 1.29$   $\mu$ M ( $n = 4$ ). The similar IC<sub>50</sub> values obtained with the two distinct protocols supported the use of the cumulative dosing approach in the SAR studies described below.

**ML204 Block of TRPC4 $\beta$  Channels Is Not Dependent upon GPCR Activation**—ML204 inhibited TRPC4 $\beta$ -mediated cation influx in both fluorescent and electrophysiological assays, in which TRPC4 $\beta$  channels were activated by the  $\mu$ -OR agonist, DAMGO. However, it was difficult to know whether the compound acted on the GPCR signaling pathways or directly on the TRPC4 channels in these assays. In order to distinguish these possibilities, we tested the ML204 effects on TRPC4 $\beta$  by activating the channel via different mechanisms.

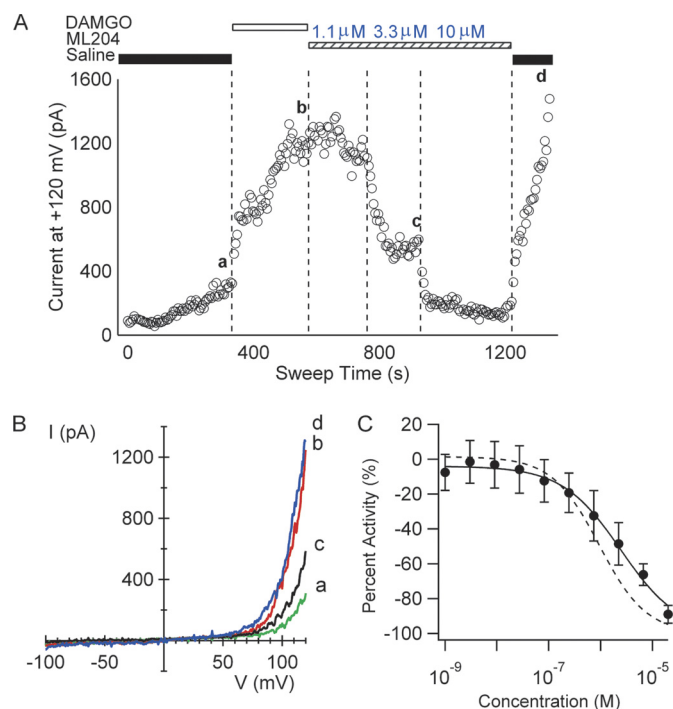


**FIGURE 3. ML204 blocks TRPC4 current elicited by different activation mechanisms.** *A*, time course of TRPC4 $\beta$  current amplitude at +120 mV for a cell exposed to intracellular solution containing 0.1 mM GTP $\gamma$ S. *B*, I-V plots of TRPC4 $\beta$  currents from the cell shown in *A*, showing traces for base line (*a*), 50 nM DAMGO (*b*), after 3.33  $\mu$ M ML204 (*c*), and after washing off ML204 and DAMGO (*d*). *C*, effect of ML204 on calcium signals in a fluorescent assay in which TRPC4 $\beta$  activation is triggered by ACh. ML204 inhibited this calcium signal with an IC<sub>50</sub> value of 2.91  $\pm$  2.1  $\mu$ M ( $n$  = 4). The dashed line is the fit to the data in Fig. 1*D*, in which the signal was triggered by DAMGO. Symbols are mean plus or minus standard deviation.

First, an automated electrophysiology assay was performed, in which GTP $\gamma$ S was included in the intracellular solution to produce persistent activation of G-proteins. As shown in Fig. 3*A*, the base-line current with GTP $\gamma$ S in the internal solution was initially at a level comparable with the currents observed using solutions lacking GTP $\gamma$ S, and the current slowly increased above the initial level (Fig. 3*A*, *a*). The addition of 50 nM DAMGO produced large and sustained increases in TRPC4 $\beta$  currents, presumably due to accelerated accumulation of activated G-proteins. The addition of ML204 in the absence of DAMGO inhibited GTP $\gamma$ S-evoked TRPC4 $\beta$  currents with an IC<sub>50</sub> value of 2.85  $\pm$  0.35  $\mu$ M ( $n$  = 4), similar to TRPC4 $\beta$  inhibition in the presence of DAMGO (Fig. 2*B*). After washout of ML204, TRPC4 currents were restored to the level prior to ML204 addition (Fig. 3*A*, *b* and *d*), indicating that the currents were independent of GPCR activation under these conditions. The similar IC<sub>50</sub> values for ML204 inhibition of TRPC4 $\beta$  currents in assays dependent on (Fig. 2) and independent of (Fig. 3, *A* and *B*) GPCR activation suggest that ML204 block of currents is not GPCR-dependent.

Second, the closely related TRPC5 channels have been shown to be partially activated by increases in [Ca<sup>2+</sup>]<sub>i</sub> (7, 25, 26). We tested whether TRPC4 $\beta$  could also be directly activated by intracellular Ca<sup>2+</sup> in TRPC4 $\beta$ / $\mu$ -OR-co-expressing cells using the automated electrophysiology instrument with intracellular solutions containing differing calculated levels of free Ca<sup>2+</sup>. Currents were elicited by voltage ramps from -100 mV

to +120 mV. Although larger currents developed at higher [Ca<sup>2+</sup>]<sub>p</sub>, current stability declined, limiting the range of [Ca<sup>2+</sup>]<sub>i</sub> that could be examined. With an estimated free [Ca<sup>2+</sup>]<sub>i</sub> of 1.8  $\mu$ M, small (<1 nA) outwardly rectifying currents were observed that were similar to the currents activated by GPCR activation in the same cells but were smaller in amplitude (not shown). ML204 (10  $\mu$ M) inhibited most of the current observed at +120 mV, although the degree of block could not be accurately quantified due to the small amplitude of the currents and difficulties in subtracting small amplitude background currents. These qualitative data further suggest a direct inhibitory effect of ML204 on TRPC4 channels.

Furthermore, TRPC4 currents were recorded using conventional (manual) patch clamp techniques from HEK293 cells co-expressing guinea pig TRPC4 $\beta$  channels and M<sub>2</sub> muscarinic receptors. ML204 (10  $\mu$ M) nearly completely blocked currents activated by 10  $\mu$ M carbachol (Fig. 4*A*). This level of inhibition is similar to the inhibition observed at 10  $\mu$ M ML204 after TRPC4 $\beta$  activation by  $\mu$ -OR activation in automated patch clamp experiments and in manual electrophysiological experiments (Fig. 4*D*).

The HEK293 cell line expressing TRPC4 $\beta$  and  $\mu$ -OR receptors also endogenously expresses G<sub>q/11</sub>-coupled muscarinic receptors, most likely the M<sub>3</sub> subtype. Application of ACh to these cells induced an intracellular calcium signal that represents a combination of transient intracellular calcium release and a sustained calcium influx signal through the expressed TRPC4 $\beta$  channels and endogenous store-operated pathways. ML204 inhibited this calcium signal with an IC<sub>50</sub> value of 2.91  $\pm$  2.1  $\mu$ M ( $n$  = 4; Fig. 3*C*), which is slightly higher than the IC<sub>50</sub> for inhibiting DAMGO-stimulated calcium flux (Fig. 3*C*, dashed line), as shown in Fig. 1*D*, and is most likely due to the inclusion of endogenous ACh-induced calcium mobilization in the calculation. In parental HEK293 cells, ML204 weakly blocked the ACh-evoked [Ca<sup>2+</sup>]<sub>i</sub> rise with an estimated IC<sub>50</sub> value greater than 30  $\mu$ M, indicating that the compound also inhibits endogenous M<sub>3</sub> muscarinic receptors in HEK293 cells, albeit at a much lower potency than its block of TRPC4 $\beta$ .

**Selectivity Profile of ML204**—Selectivity for ML204 block of different TRPC channels was evaluated in whole-cell voltage clamp recordings of HEK293 cells expressing TRPC4 $\beta$ , TRPC5, and TRPC6 channels. In cells expressing guinea pig TRPC4 $\beta$  channels along with M<sub>2</sub> muscarinic receptors, 10  $\mu$ M ML204 nearly completely blocked currents activated by 10  $\mu$ M carbachol (Fig. 4*A*), demonstrating that both mouse and guinea pig TRPC4 channels are sensitive to ML204, and the block is independent of the receptor types used to induce channel activation. In comparison, ML204 exhibited modest inhibitory effects on TRPC6 channels activated by bath application of 100  $\mu$ M carbachol to cells stably expressing mouse TRPC6 channels and transiently expressing M<sub>5</sub> muscarinic receptors (Fig. 4*B*). In these cells, M<sub>5</sub> receptors were introduced in order to obtain more consistent stimulation by carbachol. However, because ML204 shows modest inhibitory effects on muscarinic receptors, it is possible that the moderate inhibition observed in these experiments was partially mediated through the receptor rather than directly on the channel. Therefore, OAG was used to activate TRPC6 directly. Under these conditions, 10  $\mu$ M

## ML204 Selectively Modulates Native TRPC4/C5 Channels

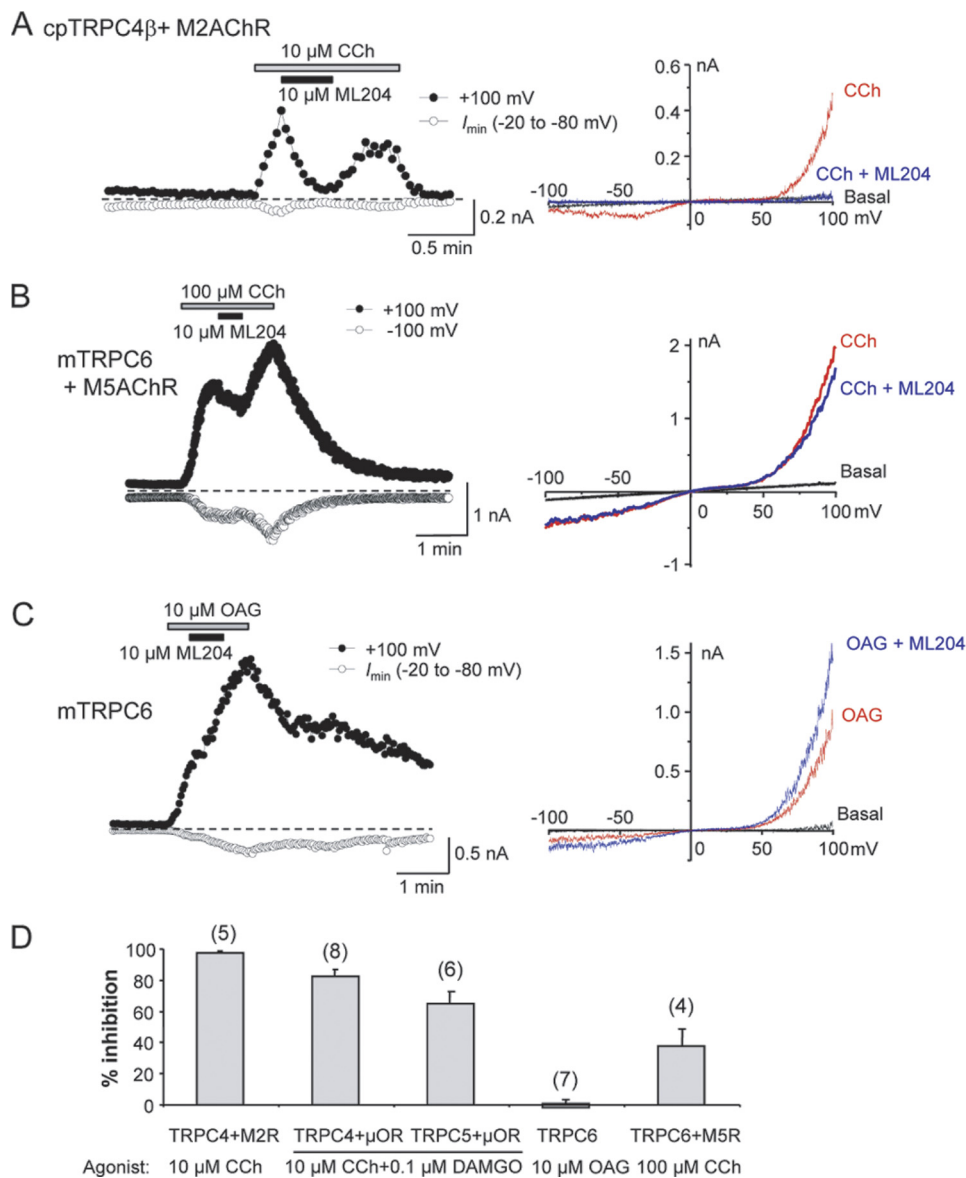


**FIGURE 4. Effect of ML204 on TRPC channels in manual whole-cell recording experiments.** *A*, HEK293 cell co-expressing guinea pig (*cp*) TRPC4 $\beta$  and M2 muscarinic receptors was voltage-clamped, and currents were elicited by voltage ramps from +100 mV to -100 mV in 100 ms. Carbachol (10  $\mu$ M) and ML204 (10  $\mu$ M) were added as indicated. *Left*, time courses of current development at +100 mV and maximal inward currents between -20 and -80 mV. *Right*, the *I-V* relationship at basal level, after carbachol stimulation, and in the presence of ML204. *B*, similar to *A*, but the cell expressed mouse TRPC6 and M5 muscarinic receptors. TRPC6 currents were activated by 100  $\mu$ M carbachol. *C*, similar to *B*, but the cell expressed mouse TRPC6 only. TRPC6 currents were activated by bath application of 10  $\mu$ M OAG. The continued increase after ML204 application is not an indication of potentiation because the currents also increased in the absence of ML204. *D*, summary of ML204 action (10  $\mu$ M) on TRPC currents evoked via different mechanisms as indicated. Cells expressed different TRPCs and GPCRs as indicated. Data are means  $\pm$  S.E. (error bars) of percentage inhibition for the numbers of cells indicated in parentheses.

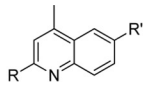
ML204 produced no appreciable block of TRPC6 currents (Fig. 4C), suggesting a lack of effect by ML204 on TRPC6 channels. A summary of ML204 effects on TRPC channels in manual electrophysiological experiments is shown in Fig. 4D. At 10  $\mu$ M, ML204 produced a nearly complete block of TRPC4 $\beta$  channels activated either through the muscarinic or  $\mu$ -opioid receptor signaling pathways. It produced  $\sim$ 65% inhibition of TRPC5 activated through  $\mu$ -OR. However, the inhibition on TRPC6 is dependent upon the mode of activation, which was  $\sim$ 38% when stimulated via M<sub>5</sub> muscarinic receptors and none with stimulation by OAG.

ML204 was evaluated for block of TRPC6 channels using a fluorescent assay measuring membrane potential changes in a

HEK293 cell line stably expressing TRPC6 channels and endogenous muscarinic receptors. TRPC6 activation was initiated following the addition of ACh to the cells, and membrane potential changes reflected cation influx through TRPC6 channels because these were not evident after ACh addition to parental HEK293 cells lacking TRPC6 channels. The membrane depolarization signal was blocked by ML204 with an IC<sub>50</sub> of 18.4  $\mu$ M (Table 1). However, because TRPC6 activation in this assay was dependent on ACh stimulation of muscarinic receptors, which itself was weakly inhibited by ML204, it is possible that some inhibitory effects observed here at high concentrations of ML204 were due to blockade of the muscarinic receptors rather than the TRPC6 channels.

TABLE 1

SAR of left- and right-hand portions of ML204 establishes the need for small cycloalkyl substitution



Cmpd	R	R'	TRPC4 mOR, $\mu\text{M}^a$ (% inhib. @ 20 $\mu\text{M}$ )	Ephys <sup>a</sup> ( $\mu\text{M}$ )	TRPC6, $\mu\text{M}^b$ (% inhib. @ 20 $\mu\text{M}$ )	Selectivity
1		H	0.96 ± 0.26	2.6 <sup>b</sup>	18.4	19
2		H	2.75 ± 0.79	8.02 ± 2.16	14.93	5.4
3		H	1.50 <sup>b</sup>	1.96 ± 0.22	9.74	6.5
4		H	5.31 ± 3.85	2.6 ± 0.95	>20	>4
5		H	12.63 <sup>b</sup>	11.9 ± 1.97	>20	~1
6		H	(-93.7 <sup>c</sup> )	nd	23.8	N/A
7		H	>20 (39.4)	>20 <sup>b</sup>	23.22	1
8		H	>20 (23.2)	nd	nd	N/A
9		H	5.24 <sup>b</sup>	7.54 ± 0.63	>20	~4
13		H	2.49 ± 0.4	5.46 ± 1.12	14.23	5.7
22		Me	5.82b	3.93b	8.58	3
23		Me	1.5 ± 0.47	3.91 ± 0.57	2.03	0.52
25		Et	(45.8)	3.73 ± 0.5	14.99	4.0
26		Et	0.58 ± 0.09	2.06 ± 0.2	4.24	7.3
28		F	10.50b	6.38 ± 0.26	20.21	2
29		F	1.05 ± 0.28	3.94 ± 0.16	7.15	7

<sup>a</sup> The  $\text{IC}_{50}$  is the average of at least three independent titrations (mean ± S.D. Shown in the table) by automated electrophysiological recording.

<sup>b</sup> The  $\text{IC}_{50}$  is either the result of a group fit or a single dose titration.

<sup>c</sup> Compounds with <50% inhibition at 20  $\mu\text{M}$  were not further profiled for  $\text{IC}_{50}$  data indicated by nd.

Selectivity of ML204 inhibition of non-TRPC channels was determined using a combination of electrophysiological and fluorescent assays. ML204 at 10  $\mu\text{M}$  caused no significant inhibition (<20%) of TRPV1 channels activated by the addition of 30 nM capsaicin and at 30  $\mu\text{M}$  no significant inhibition (10% change) of KCNQ2 potassium channels in automated electrophysiological experiments (not shown).

The effects of ML204 on a panel of TRP channels were evaluated using FlexStation assays monitoring changes in fluorescent intensity due to changes in  $[\text{Ca}^{2+}]_i$  measured with Fluo4. A series of ML204 concentrations, up to 22.2  $\mu\text{M}$ , caused no inhibition of the responses of TRPA1, TRPM8, TRPV1, or TRPV3 to corresponding agonists. High concentrations of ML204 caused very weak and slow activation of TRPA1 (supplemental Fig. S1).

Effects of ML204 on voltage-gated sodium, potassium, and calcium channels were evaluated using whole-cell voltage clamp recordings from neurons isolated from mouse dorsal root ganglia. ML204 at 10  $\mu\text{M}$  exhibited no significant inhibition (<10%) of these currents (supplemental Fig. S2). Individual current recordings and  $I$ - $V$  relations in the presence of

TABLE 2

Ricerca profiling of ML204

Compound	Primary Biochemical Assay	Species	% inhibition @ 10 $\mu\text{M}$
ML204	Adrenergic, $\alpha_{1A}$	rat	54%
	Adrenergic, $\alpha_{2A}$	human	58%
	Histamine, $H_1$	human	77%
	Imidazole $I_2$ , central	rat	77%
	Muscarinic, $M_2$	human	61%
	Nicotinic acetylcholine	human	76%
	Sigma, $\sigma_1$	human	83%

ML204 were identical with control recordings from the same cells.

ML204 was also examined in broad profiling studies. ML204 was tested in 397 assays listed in PubChem and was active in only one assay (cycloheximide counter screen for small molecule inhibitors of Shiga toxin, AID 2314) that is not TRPC4-based. Furthermore, ML204 was tested at Ricerca's (formerly MDS Pharma's) Lead Profiling Screen (binding assay panel of 68 GPCRs, ion channels, and transporters screened at 10  $\mu\text{M}$ ) and was found to not significantly interact with 61 of the 68 assays conducted (with the criterion of no inhibition of radioligand binding greater than 50% at 10  $\mu\text{M}$ ). ML204 did have activity against several targets (Table 2); however, it should be pointed out that these are only single-point values and that functional selectivity may differ from binding study results.

**ML204 Blocks Muscarinic Receptor-activated Cation Channels in Intestinal Smooth Muscle Cells**—The relatively high selectivity for TRPC4 suggests that ML204 would be effective on the native channels. It has been previously shown that TRPC4 and TRPC6 channels mediate the  $mI_{\text{CAT}}$  in intestinal smooth muscle cells, with TRPC4 being the major component, accounting for 80% of  $mI_{\text{CAT}}$  in mouse ileal myocytes (17). To test if ML204 single smooth muscle myocytes inhibits endogenous TRPC4 channels,  $mI_{\text{CAT}}$  was activated in freshly isolated from guinea pig ileum either with bath application of carbachol (100  $\mu\text{M}$ ; peak current density was  $-8.3 \pm 2.3$  pA/pF at  $-40$  mV,  $n = 9$ ) (Fig. 5A) or intracellular infusion of GTP $\gamma$ S (200  $\mu\text{M}$ , peak current density was  $-9.7 \pm 1.2$  pA/pF at  $-40$  mV,  $n = 10$ ) (Fig. 5B). Application of ML204 (10  $\mu\text{M}$ ) significantly blocked the carbachol-evoked currents by  $86 \pm 2\%$  ( $n = 9$ ) and GTP $\gamma$ S-induced current by  $65 \pm 4\%$  ( $n = 10$ ) (Fig. 5C). Less than complete block is in part due to co-activation of ML204-insensitive TRPC6 channels in this functional assay (17). The level of inhibition is consistent with the data from knock-out mice (see "Discussion"). Hence, this result supports use of ML204 as a specific TRPC4 probe in native tissues.

**SAR Studies**—Analogues of ML204 were synthesized and/or purchased to determine the components of ML204 that contribute to inhibition of TRPC4 $\beta$  channels. Effects of compounds on TRPC4 $\beta$  channels were analyzed using the fluorescent assay as shown in Fig. 1 and confirmed for a subset of compounds using a QPatch electrophysiological assay. Selectivity against block of ACh-induced TRPC6 channel response was also performed using the fluorescent membrane potential assay. The original hit (1) was resynthesized and confirmed at 0.96  $\mu\text{M}$  against TRPC4 with ~19-fold selectivity over ACh-induced TRPC6 activation. The initial SAR surrounded modification of the left side (R-group) (Table 1 and Fig. 6). The most potent analogs were the original hit (piperidine), the five-mem-



## ML204 Selectively Modulates Native TRPC4/C5 Channels

bered ring analog (**2**; 2.75  $\mu\text{M}$ ,  $\sim$ 5.4-fold selectivity), and the seven-membered ring analog (**3**; 1.50  $\mu\text{M}$ , 9.7-fold selective). The SAR around this scaffold was rather steep because substituted piperidine analogs were much less active (**4** (5.3  $\mu\text{M}$ ) and **5** (12.6  $\mu\text{M}$ )). The addition of heteroatoms was also not well tolerated (morpholine, **7** (>20  $\mu\text{M}$ ) and piperidine, **6** (inactive)). Substitutions with larger aryl groups were also not well tolerated. The diethyl amine (**9**; 5.2  $\mu\text{M}$ ) led to a  $\sim$ 5-fold loss of activity; however, methyl substitution on the pyrrolidine was tolerated (**13**; 2.5  $\mu\text{M}$ ), which was equipotent with the unsubstituted compound (see supplemental Tables S1 and S2 for full SAR analysis).

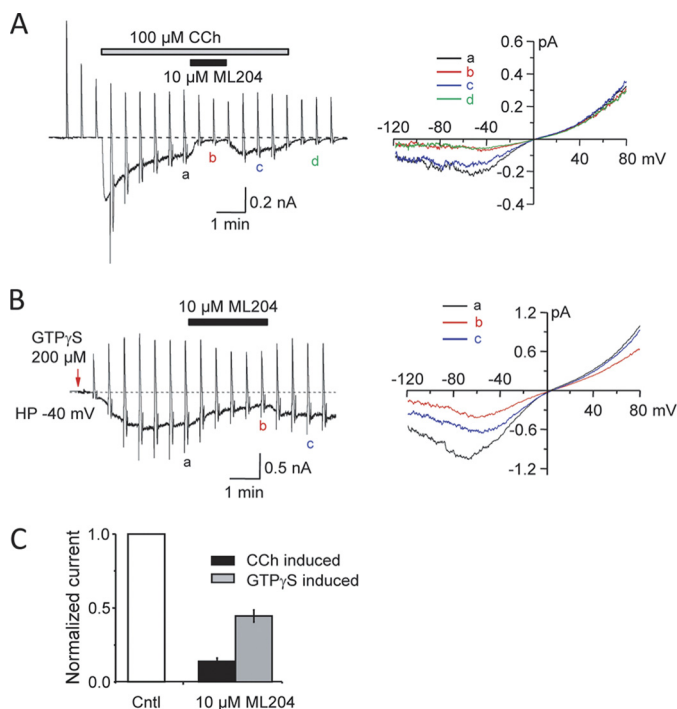


**FIGURE 5. Inhibition of endogenous  $mI_{\text{CAT}}$  in intestinal smooth muscle cells by ML204.** *A*, effect of ML204 on carbachol (CCh)-induced  $mI_{\text{CAT}}$ . *Left*, time course of the experiment showing  $mI_{\text{CAT}}$  development in response to 100  $\mu\text{M}$  CCh and reversible current inhibition by ML204 (10  $\mu\text{M}$ ). Current desensitization prevents complete current recovery after drug wash-out. *Vertical deflections* on the trace are caused by voltage ramps applied at 30-s intervals in order to measure steady-state  $I$ - $V$  relationships. *Right*,  $mI_{\text{CAT}}$   $I$ - $V$  relationships measured in control (*a*), in the presence of ML204 (10  $\mu\text{M}$ ) (*b*), and after wash-out of ML204 (*c*) and CCh (*d*), as denoted on the *left*. *B*, effect of ML204 on GTP $\gamma$ S-induced  $mI_{\text{CAT}}$ ; similar to *A*, but the current was induced by intracellular infusion of GTP $\gamma$ S (200  $\mu\text{M}$ ). The *arrow* indicates the time of membrane break-through. *HP*, holding potential. *C*, summary of ML204 on  $mI_{\text{CAT}}$  activated by either CCh (100  $\mu\text{M}$ ) or intracellular infusion of GTP $\gamma$ S (200  $\mu\text{M}$ ). The mean current density (normalized as 1) immediately before ML204 application (holding potential of  $-40$  mV) was  $-8.27 \pm 2.29$  pA/pF ( $n = 9$ ) and  $-9.71 \pm 1.18$  pA/pF ( $n = 10$ ) for CCh and GTP $\gamma$ S, respectively. *Error bars* are plus or minus standard error.

Having established the most potent left-hand substituents (piperazine, pyrrolidine, and homopiperazine), a library synthesis of these compounds was initiated ( $3 \times 8$ ) in order to further explore the quinoline portion of the molecule (Table 1 and Fig. 6). When varying the right side, the pyrrolidine analog proved to be more active than the piperidine (**22** (5.8  $\mu\text{M}$ ) versus **23** (1.5  $\mu\text{M}$ ), **26** (0.58  $\mu\text{M}$ ) versus **25** (>20  $\mu\text{M}$ ), and **29** (1.05  $\mu\text{M}$ ) versus **28** (10.5  $\mu\text{M}$ )). Of note, **26** was the most active compound tested (0.58  $\mu\text{M}$ ); however, the compound is not as selective ( $\sim$ 7.3-fold) against ACh-induced TRPC6 activation compared with **1**. Substitution is not tolerated in the 4-position of the quinoline ring or the 8-position. In addition, removal of the phenyl ring of the quinoline (pyridine or pyrimidine) is also not tolerated. Substitution of the 6-position is tolerated for some compounds. For example, ethyl substitution is not tolerated when R is piperidine (**1** versus **25**); however, ethyl substitution enhances the potency when R is pyrrolidine (**2** versus **26**). We have evaluated both portions of the primary hit (left-hand amine substituent and the right-hand quinoline) and have determined the SAR to be rather steep for this molecule. Small cycloalkyl ring moieties are tolerated on the left-hand portion, and very limited substitution is tolerated on the quinoline.

## DISCUSSION

We report here the first potent and selective blocker for TRPC4 channels, ML204, with apparent  $\text{IC}_{50}$  values of about 1  $\mu\text{M}$  in fluorescent intracellular  $\text{Ca}^{2+}$  assays and about 3  $\mu\text{M}$  in whole-cell voltage clamp experiments. ML204 blocked TRPC4 $\beta$  activity induced through either  $G_{i/o}$  stimulation by  $\mu$ -opioid, 5HT $_{1A}$  serotonin, and  $M_2$  muscarinic receptors or  $G_{q/11}$  stimulation by the endogenous  $M_3$ -like muscarinic receptors. It also blocked TRPC4 $\beta$  channels activated by intracellularly applied GTP $\gamma$ S or  $\text{Ca}^{2+}$ , which bypass receptor stimulation. These results point to a direct inhibitory effect of ML204 on TRPC4 $\beta$  channels, although effects on modulatory components closely coupled to TRPC4 $\beta$  channels cannot be excluded.

**Selectivity**—ML204 exhibited some selectivity within the TRPC subfamily of channels and higher selectivity against other TRP channels and non-TRP channels. ML204 inhibited TRPC5 channel currents activated through co-stimulation of  $G_{i/o}$  and  $G_{q/11}$  signaling by  $\mu$ -opioid and  $M_3$ -like muscarinic receptors. This result is not surprising, given the close similarity between TRPC5 and TRPC4 channels. On the other hand, the effects of ML204 on TRPC6 are uncertain. In membrane potential assays, the compound blocked carbachol-induced membrane depolarization mediated by TRPC6 with an  $\text{IC}_{50}$  of  $\sim$ 19  $\mu\text{M}$ , and in whole-cell manual electrophysiological recordings,

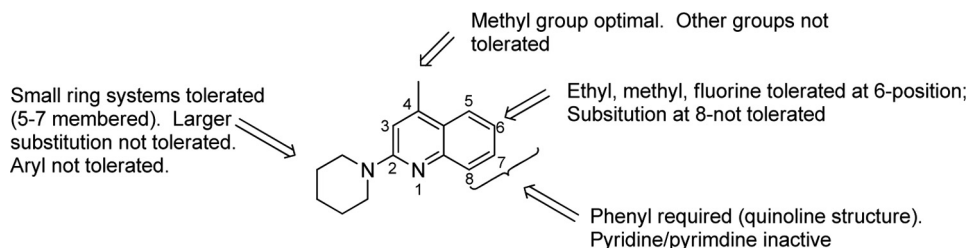


**FIGURE 6. SAR and lead optimization summary of ML204, 1.** Shown is a summary of observed SAR of over 45 analogs synthesized examining all regions of **1**.

10  $\mu\text{M}$  ML204 inhibited carbachol-evoked TRPC6 currents in cells co-expressing  $M_5$  muscarinic receptors by about 40%. However, given that ML204 weakly inhibited endogenous  $G_{q/11}$ -coupled muscarinic responses in parental HEK293 cells, the inhibition by ML204 of the carbachol-induced TRPC6 activity could be, at least partially, attributed to block of receptor signaling. Interestingly, ML204 at 10  $\mu\text{M}$  did not affect TRPC6 whole-cell currents activated via bath application of OAG, a direct activator of TRPC6 (5), suggesting a lack of direct effect of this compound on TRPC6 channels. Further investigations are needed to evaluate the roles of ML204 on TRPC6 and other TRPC channels of the non-TRPC4/C5 subgroup, which share only about 40% sequence identity with TRPC4/C5.

The selectivity of ML204 was further confirmed by the lack of effect of this compound on heterologously expressed TRP channels of other subfamilies, including TRPV1, TRPV3, TRPM8, and TRPA1, as well as non-TRP channels (e.g. expressed KCNQ2 potassium channels and native voltage-gated sodium, potassium, and calcium channels expressed in mouse dorsal root ganglion neurons). In broad profiling studies, ML204 at 10  $\mu\text{M}$  showed >50% inhibition in only 7 of 68 binding assays for 68 GPCRs, ion channels, and transporters. Therefore, ML204 appears to afford excellent selectivity for TRPC4 and TRPC5. The selectivity profile of ML204 is superior to the currently available TRPC channel blockers, SKF96365, 2-aminoethoxydiphenyl borate, and flufemanic acid, which are known to affect voltage-gated channels, intracellular  $\text{Ca}^{2+}$  release channels, chloride channels, and/or multiple types of TRP channels from several subfamilies (5, 27, 28).

TRPC4 and TRPC5 are abundantly expressed in smooth muscle and central nervous system, but these expression patterns do not perfectly overlap (29, 30). TRPC channels can function as both homo- and heterotetramers with a preference of heteromultimerization among members of the same TRPC subgroup, as well as TRPC1 with TRPC4/C5 (31–33). However, evidence for coassembly between TRPC3 and TRPC1 or TRPC4 has also been reported (34–36). Coassembly of different TRPC subunits is probably cell-specific and developmentally regulated (32), providing a diversity of functional TRPC channels. It would be important to perform detailed analyses evaluating how ML204 acts on heteromultimeric channels.

Importantly, ML204 blocked the native  $mI_{\text{CAT}}$  in smooth muscle myocytes freshly isolated from guinea pig ileum. This well characterized current response has many features that resemble those of TRPC, especially TRPC4/C5, channels, including dependence on G protein signaling,  $I$ - $V$  relationships, calcium modulation, and potentiation by lanthanides (22, 37, 38). Indeed,  $mI_{\text{CAT}}$  was reduced by 80% in ileal smooth muscle cells isolated from TRPC4 knock-out mice, and the remaining current was eliminated by further knock-out of TRPC6 (17). In the current study, 10  $\mu\text{M}$  ML204 reduced carbachol-induced  $mI_{\text{CAT}}$  by >85% and GTP $\gamma$ S-induced currents by ~65%. Although both activation protocols cause activation of TRPC4 and TRPC6, the GTP $\gamma$ S-induced activation does not involve muscarinic receptors. Therefore, because of the moderate inhibitory effect of ML204 on muscarinic receptors, the TRPC6 fraction of the  $mI_{\text{CAT}}$  would be partially inhibited when activation was induced by carbachol but not when it was induced by

GTP $\gamma$ S, assuming that TRPC6 is insensitive to the blocker. This may explain the different degrees of ML204 block of  $mI_{\text{CAT}}$  activated by carbachol and GTP $\gamma$ S. However, it cannot be ruled out that GTP $\gamma$ S has other effects differing from carbachol on current activation in guinea pig ileal myocytes that are insensitive to ML204. Overall, the data support that ML204 specifically inhibits the TRPC4 components of  $mI_{\text{CAT}}$  in intestinal smooth muscle cells. Although RNA interference experiments to knockdown  $mI_{\text{CAT}}$  current in these cells would be interesting, the combined loss of smooth muscle properties makes such experiments unfeasible.

An important feature of  $mI_{\text{CAT}}$  is that it requires simultaneous activation of both  $M_2$  and  $M_3$  muscarinic receptors (i.e. co-stimulation of both  $G_{i/o}$  and  $G_{q/11}$  signaling) (22), a property not particularly well known for expressed TRPC channels. Nonetheless, the activation of TRPC4 by GTP $\gamma$ S infusion is blocked by pertussis toxin (24), and co-expression of  $G\alpha_i$  proteins with TRPC4 supports channel activation (8), demonstrating the role of  $G_{i/o}$  proteins in facilitating TRPC4/C5 activation. Hence,  $\mu$ -OR stimulation was used as a convenient way to trigger TRPC4 channel activation in a fluorescence  $\text{Ca}^{2+}$  assay with minimal background response in the primary high throughput screen (20). This assay afforded excellent signal-to-background ratios and  $Z'$  factors in the fluorescence assay in microplate format. However, in whole-cell recordings, activation of  $G_{i/o}$  signaling alone leads to only weak stimulation of the TRPC4 currents. Therefore, in the automated patch clamp experiments, the stimulated currents displayed mostly outward currents at positive potentials, representing moderate channel activation, consistent with voltage dependence at positive potentials. Despite being partially active, this level of activation is more sustained and stable, suitable for high throughput sample analysis of the automated electrophysiological system. In manual patch clamp experiments, we have stimulated TRPC4 and TRPC5 by co-activation of both  $G_{i/o}$ - and  $G_{q/11}$ -coupled receptors, producing very strong channel activation. Under these conditions, the voltage dependence of the channel is more negatively shifted, giving rise to the U-shaped  $I$ - $V$  relationship in the negative potential range, typical for  $mI_{\text{CAT}}$  (22). The precise shape of the  $I$ - $V$  curve is affected by the solution compositions and voltage protocols. Specifically, only when ramping from positive to negative voltages for long durations (seconds) can the quasi-steady state currents be reviewed at different potentials and therefore the perfect U-shaped  $I$ - $V$  (39). Therefore, in the current study, the  $I$ - $V$  curves of TRPC4 currents activated under different conditions appear different. Despite this, the inhibitory effect of ML204 was observed under all conditions, demonstrating that ML204 is a potent blocker of the TRPC4 channels.

The initial efforts of synthesis and biological characterization of ML204 displayed a relatively flat SAR. Substitution at the 2-position revealed that small heterocycloalkyl substituents were the most tolerated (piperidine and pyrrolidine). Substitution of the 4-methyl (trifluoromethyl/phenyl) led to a loss of potency. Alkyl and halogen substitutions were tolerated at the 6-position, but selectivity *versus* ACh-induced TRPC6 activation suffered. Last, deletion of the right-hand phenyl (i.e. substituted pyridine or pyrimidine) led to inactive compounds.

## ML204 Selectively Modulates Native TRPC4/C5 Channels

The SAR studies have identified a higher affinity analog, compound 26. Although this compound is less discriminative for TRPC6, it is possible that its high potency may be useful in certain analyses, for example in generating a radioactive TRPC4 ligand in heterologous binding studies.

In summary, using a high throughput screen of the MLSMR library, we have identified and characterized a potent and selective TRPC4/C5 antagonist, ML204. Although the compound also has some weak inhibitory effects on muscarinic and other G protein-coupled receptors, it displays at least 20-fold higher selectivity for TRPC4 over a collection of other related and non-related ion channels and receptors, including TRPC6 within the same TRPC subfamily, and members of other TRP subfamilies, such as TRPV1, TRPV3, TRPM8, and TRPA1. This level of selectivity is far superior to other pharmacological blockers currently used in TRPC channel research and should provide specific blockade of TRPC4/C5 channels in native tissues in physiological studies, hence complementing studies using siRNA knockdown, gene knock-out, or blocking antibodies. It is anticipated that the new TRPC4 blocker will have a wide use in physiological and pathophysiological studies for delineating the functional significance of the TRPC4/C5 channels and facilitate the development of therapeutics targeted to TRPC channels.

*Acknowledgment—We thank Alison Neal for editorial assistance.*

### REFERENCES

- Clapham, D. E. (2003) *Nature* **426**, 517–524
- Montell, C., Birnbaumer, L., and Flockerzi, V. (2002) *Cell* **108**, 595–598
- Plant, T. D., and Schaefer, M. (2003) *Cell Calcium* **33**, 441–450
- Huang, J., Liu, C. H., Hughes, S. A., Postma, M., Schwiening, C. J., and Hardie, R. C. (2010) *Curr. Biol.* **20**, 189–197
- Hofmann, T., Obukhov, A. G., Schaefer, M., Harteneck, C., Gudermann, T., and Schultz, G. (1999) *Nature* **397**, 259–263
- Ju, M., Shi, J., Saleh, S. N., Albert, A. P., and Large, W. A. (2010) *J. Physiol.* **588**, 1419–1433
- Schaefer, M., Plant, T. D., Obukhov, A. G., Hofmann, T., Gudermann, T., and Schultz, G. (2000) *J. Biol. Chem.* **275**, 17517–17526
- Jeon, J. P., Lee, K. P., Park, E. J., Sung, T. S., Kim, B. J., Jeon, J. H., and So, I. (2008) *Biochem. Biophys. Res. Commun.* **377**, 538–543
- Freichel, M., Suh, S. H., Pfeifer, A., Schweig, U., Trost, C., Weissgerber, P., Biel, M., Philipp, S., Freise, D., Droogmans, G., Hofmann, F., Flockerzi, V., and Nilius, B. (2001) *Nat. Cell Biol.* **3**, 121–127
- Philipp, S., Hambrecht, J., Braslavski, L., Schroth, G., Freichel, M., Murakami, M., Cavalié, A., and Flockerzi, V. (1998) *EMBO J.* **17**, 4274–4282
- Jung, S., Mühle, A., Schaefer, M., Strotmann, R., Schultz, G., and Plant, T. D. (2003) *J. Biol. Chem.* **278**, 3562–3571
- Zeng, F., Xu, S. Z., Jackson, P. K., McHugh, D., Kumar, B., Fountain, S. J., and Beech, D. J. (2004) *J. Physiol.* **559**, 739–750
- Tirupathi, C., Freichel, M., Vogel, S. M., Paria, B. C., Mehta, D., Flockerzi, V., and Malik, A. B. (2002) *Circ. Res.* **91**, 70–76
- Munsch, T., Freichel, M., Flockerzi, V., and Pape, H. C. (2003) *Proc. Natl. Acad. Sci. U.S.A.* **100**, 16065–16070
- Freichel, M., Vennekens, R., Olausson, J., Stolz, S., Philipp, S. E., Weissgerber, P., and Flockerzi, V. (2005) *J. Physiol.* **567**, 59–66
- Lee, K. P., Jun, J. Y., Chang, I. Y., Suh, S. H., So, I., and Kim, K. W. (2005) *Mol. Cells* **20**, 435–441
- Tsvilovskyy, V. V., Zholos, A. V., Aberle, T., Philipp, S. E., Dietrich, A., Zhu, M. X., Birnbaumer, L., Freichel, M., and Flockerzi, V. (2009) *Gastroenterology* **137**, 1415–1424
- Boulay, G., Zhu, X., Peyton, M., Jiang, M., Hurst, R., Stefani, E., and Birnbaumer, L. (1997) *J. Biol. Chem.* **272**, 29672–29680
- Hu, H., Tian, J., Zhu, Y., Wang, C., Xiao, R., Herz, J. M., Wood, J. D., and Zhu, M. X. (2010) *Pflugers Arch.* **459**, 579–592
- Miller, M., Wu, M., Xu, J., Weaver, D., Li, M., and Zhu, M. X. (2011) in *TRP Channels* (Zhu, M. X., ed) pp. 1–20, CRC Press, Inc., Boca Raton, FL
- Malin, S. A., Davis, B. M., and Molliver, D. C. (2007) *Nat. Protoc.* **2**, 152–160
- Zholos, A. V., and Bolton, T. B. (1997) *Br. J. Pharmacol.* **122**, 885–893
- Hu, H. Z., Gu, Q., Wang, C., Colton, C. K., Tang, J., Kinoshita-Kawada, M., Lee, L. Y., Wood, J. D., and Zhu, M. X. (2004) *J. Biol. Chem.* **279**, 35741–35748
- Otsuguro, K., Tang, J., Tang, Y., Xiao, R., Freichel, M., Tsvilovskyy, V., Ito, S., Flockerzi, V., Zhu, M. X., and Zholos, A. V. (2008) *J. Biol. Chem.* **283**, 10026–10036
- Blair, N. T., Kaczmarek, J. S., and Clapham, D. E. (2009) *J. Gen. Physiol.* **133**, 525–546
- Gross, S. A., Guzmán, G. A., Wissenbach, U., Philipp, S. E., Zhu, M. X., Bruns, D., and Cavalié, A. (2009) *J. Biol. Chem.* **284**, 34423–34432
- Inoue, R., Okada, T., Onoue, H., Hara, Y., Shimizu, S., Naitoh, S., Ito, Y., and Mori, Y. (2001) *Circ. Res.* **88**, 325–332
- Merritt, J. E., Armstrong, W. P., Benham, C. D., Hallam, T. J., Jacob, R., Jaxa-Chamiec, A., Leigh, B. K., McCarthy, S. A., Moores, K. E., and Rink, T. J. (1990) *Biochem. J.* **271**, 515–522
- Beech, D. J., Muraki, K., and Flemming, R. (2004) *J. Physiol.* **559**, 685–706
- Fowler, M. A., Sidiropoulou, K., Ozkan, E. D., Phillips, C. W., and Cooper, D. C. (2007) *PLoS One* **2**, e573
- Hofmann, T., Schaefer, M., Schultz, G., and Gudermann, T. (2002) *Proc. Natl. Acad. Sci. U.S.A.* **99**, 7461–7466
- Strübing, C., Krapivinsky, G., Krapivinsky, L., and Clapham, D. E. (2003) *J. Biol. Chem.* **278**, 39014–39019
- Yuan, J. P., Kiselyov, K., Shin, D. M., Chen, J., Shcheynikov, N., Kang, S. H., Dehoff, M. H., Schwarz, M. K., Seeburg, P. H., Muallem, S., and Worley, P. F. (2003) *Cell* **114**, 777–789
- Lintschinger, B., Balzer-Geldsetzer, M., Baskaran, T., Graier, W. F., Romanin, C., Zhu, M. X., and Groschner, K. (2000) *J. Biol. Chem.* **275**, 27799–27805
- Liu, X., Bandyopadhyay, B. C., Singh, B. B., Groschner, K., and Ambudkar, I. S. (2005) *J. Biol. Chem.* **280**, 21600–21606
- Poteser, M., Graziani, A., Rosker, C., Eder, P., Derler, I., Kahr, H., Zhu, M. X., Romanin, C., and Groschner, K. (2006) *J. Biol. Chem.* **281**, 13588–13595
- Inoue, R., Morita, H., Yanagida, H., and Ito, Y. (1998) *J. Smooth Muscle Res.* **34**, 69–81
- Inoue, R., and Isenberg, G. (1990) *J. Physiol.* **424**, 73–92
- Zholos, A. V., Zholos, A. A., and Bolton, T. B. (2004) *J. Gen. Physiol.* **123**, 581–598